communications biology

Article

https://doi.org/10.1038/s42003-024-06576-w

Eddy-driven diazotroph distribution in the subtropical North Atlantic: horizontal variability prevails over particle sinking speed

Check for updates

E. Cerdán-García [1,2] ✉, X. A. Álvarez-Salgado[3], J. Arístegui [4], A. Martínez-Marrero [4] & M. Benavides [1,2] ✉

Mesoscale eddies influence the distribution of diazotrophic (nitrogen-fixing) cyanobacteria, impacting marine productivity and carbon export. Non-cyanobacterial diazotrophs (NCDs) are emerging as potential contributors to marine nitrogen fixation, relying on organic matter particles for resources, impacting nitrogen and carbon cycling. However, their diversity and biogeochemical importance remain poorly understood. In the subtropical North Atlantic along a single transect, this study explored the horizontal and vertical spatial variability of NCDs associated with suspended, slow-sinking, and fast-sinking particles collected with a marine snow catcher. The investigation combined amplicon sequencing with hydrographic and biogeochemical data. Cyanobacterial diazotrophs and NCDs were equally abundant, and their diversity was explained by the structure of the eddy. The unicellular symbiotic cyanobacterium UCYN-A was widespread across the eddy, whereas *Trichodesmium* and *Crocosphaera* accumulated at outer fronts. The diversity of particle-associated NCDs varied more horizontally than vertically. NCDs constituted most reads in the fast-sinking fractions, mainly comprising Alphaproteobacteria, whose abundance significantly differed from the suspended and slow-sinking fractions. Horizontally, Gammaproteobacteria and Betaproteobacteria exhibited inverse distributions, influenced by physicochemical characteristics of water intrusions at the eddy periphery. Niche differentiations across the anticyclonic eddy underscored NCD-particle associations and mesoscale dynamics, deepening our understanding of their ecological role and impact on ocean biogeochemistry.

The availability of nitrogen (N) is one of the crucial limiting factors constraining the growth and activity of phytoplankton, which in turn has major roles in primary production and biogeochemical cycling in the ocean[1]. Through the process of dinitrogen (N_2) fixation, prokaryotic microbes termed 'diazotrophs' convert molecular N_2 into reactive N forms, representing the main source of new N in the open ocean[2]. Diazotrophs are predominantly composed of photosynthetic cyanobacteria including the filamentous colony-forming *Trichodesmium*, or the unicellular symbiont UCYN-A. However, recent studies highlighted non-cyanobacterial diazotrophs (NCDs) as potentially important contributors to the supply of new N in marine ecosystems (reviewed in refs. 3,4). NCD phylogenetic groups including alpha-, beta-, gamma- and delta- from the phylum proteobacteria are widely distributed across the ocean[5,6]. Unlike light-dependent cyanobacteria, NCDs are mostly described as heterotrophs[3,7] obtaining carbon and energy from organic matter respiration. Some also exhibit complex metabolic traits like photoheterotrophy, or chemolithotrophy[4]. However, most of our knowledge on NCDs derives from amplicon or genomic studies, and little is known about their ecology and contribution to N_2 fixation in the ocean.

[1]Aix Marseille Université, CNRS, Université de Toulon, IRD, OSU Pythéas, Mediterranean Institute of Oceanography (MIO), UM 110, 13288 Marseille, France. [2]Turing Centre for Living Systems, Aix-Marseille University, 13009 Marseille, France. [3]Instituto de Investigacións Mariñas (CSIC), Vigo, Spain. [4]Instituto de Oceanografía y Cambio Global (IOCAG), Universidad de Las Palmas de Gran Canaria, ULPGC, Gran Canaria, Spain. ✉e-mail: elena.cerdan@mio.osupytheas.fr; mar.benavides@noc.ac.uk

Both cyanobacterial diazotrophs and NCDs have been observed associated with particles below the euphotic zone, with different sinking rates according to their phylogenetic group[8]. Some diazotroph cyanobacteria such as *Crocosphaera* (UCYN-B) produce polysaccharides, which help individual cells to aggregate into larger particulate forms[9]. On the other hand, some NCD groups have been found in large filter size fractions, presumably adopting particle-associated lifestyles[7,10,11]. Particles are thought to provide NCDs with conditions favourable for N_2 fixation[12]. High respiration rates may generate anaerobic microenvironments within particles, which, together with the high carbon-to-nitrogen (C:N) ratio exceeding the Redfield ratio (106:16) and the availability of labile carbon in the aggregate material, are key conditions for N_2 fixation[13,14]. Emerging compilations of NCD amplicon and metagenomic databases (e.g. ref. 4) are bringing efforts together to establish a wider spectrum of the diversity and capacities of these microorganisms on a global scale. Additionally, despite all this inferred evidence, there is no information regarding how the association of NCDs with particles occurs, what factors drive these associations (e.g., particle density, composition, sinking speed) or if specific NCD groups prefer one type of particle over another. Hence a more comprehensive understanding of the spatio-temporal dynamics of particle-associated NCDs in the ocean is needed.

Mesoscale eddies play a crucial role in particle distribution dynamics, influencing ocean biogeochemistry. Eddies can pump water vertically, either supplying nutrients to enhance primary productivity or subducting surface biomass, promoting export[15]. Anticyclonic eddies tend to decrease biological production in their interior by causing downwelling, while cyclonic eddies uplift isopycnals inducing upwelling and enhancing chlorophyll and nutrients at their surface[15]. Eddies are important in pelagic nitrogen cycling, with anticyclonic eddies influencing diazotroph accumulation and N_2 fixation rates[16–19]. Despite their impact on microbial communities, generalising eddy behaviour across ocean regions remains debated, and the physicochemical impact of mesoscale dynamics on diazotroph activity and distribution is still unclear[20].

South of the Canary Islands archipelago (subtropical Northeast Atlantic), eddies are generated year round by the perturbation of the mean flow by the islands, although they are more intense during the peak in the Trade Winds season (spring and summer), due to the interaction between oceanic and atmospheric flows[21,22]. Cyclonic and anticyclonic eddies are sequentially spun off from the islands, drifting south-westwards along the Canary Eddy Corridor (CEC) and persisting for months[23]. Eventually, eddies may interact with each other and with upwelling filaments along the African coast, leading to frontal zones of ageostrophic secondary circulation[24]. Mixing at these fronts facilitates the exchange of biogeochemical properties between coastal and open ocean waters, contributing to organic matter export[25,26].

Despite recent hypothesis regarding the association of NCDs with particles[4,10,13], there is no knowledge related to the associations or preferences for particle types of these organisms. Therefore, this study investigated the community composition of NCDs in different particles grouped by sinking speed (suspended, slow-sinking and fast-sinking). The relative abundance of cyanobacterial diazotrophs and NCDs was analysed across a mesoscale anticyclonic eddy named "*Bentayga*" in November-December 2022. This eddy was formed five months prior, originating south of Gran Canaria Island. At the time of this study, the core was located in the path of the CEC, approximately 200 km south of the islands. Differences in particle composition and sinking speed underlined both horizontal and vertical variations in diazotroph community structure. However, spatial variation in diversity was mostly explained by the horizontal structure of the eddy. Within cyanobacterial diazotrophs, UCYN-A was abundant indiscriminately throughout the anticyclonic eddy, while *Trichodesmium* and *Crocosphaera* accumulated at the peripheric frontal zones. NCDs showed dominance of Gammaproteobacteria in the east, Betaproteobacteria in the west, and Alphaproteobacteria in the fast-sinking fractions. By combining amplicon sequencing with hydrographic and biogeochemical data, the horizontal and vertical spatial variability of these groups provided a deeper understanding of the interplay between mesoscale dynamics and NCD association with particles.

Results

Oceanographic setting

The anticyclonic eddy spanned approximately 150 km in width and was characterised by a warm water core (Fig. 1). The eddy exhibited rigid rotation between stations 15 and 20, establishing them as the core (Fig. 1c). Station 18 was identified as the centre of the eddy, which was surrounded by an inner ring (stations 20–23 and 13–15) and an outer ring (stations 23–26 and 12–13) (Fig. 1c).

Additionally, the eddy embedded two filaments of colder water in its periphery (Fig. 1a), rotating slowly clockwise as it moved south-westward. The filament stretching from the northwest African coastal upwelling (Fig. 1a) was more intense, hence resulting in a more pronounced front in the east. Consequently, temperatures at the sampling depths were below 19 °C in the east, gradually increasing to near 23 °C in the west (Fig. 1b; Supplementary Table S1). At the sampling depths measured inorganic nitrogen (nitrate -NO_3^--, ammonium -NH_4^+-, total inorganic nitrogen -TIN-) and silicate (SiO_4^{4-}) showed three times higher concentrations in the eastern front (stations 2, 5) and remained constant throughout the core and western front (Supplementary Fig. S1; Supplementary Table S2). However, nitrite -NO_2^-showed a peak at station 2 and high values at stations 7, as well as in the core stations 15,18 and inner ring station 21. Phosphate -PO_4^{3-}- showed a peak at core stations 15–21, and a decrease on the western front (Supplementary Fig. S1; Supplementary Table S2).

Environmental variability across the eddy

A principal component analysis (PCA) including the physicochemical parameters revealed significant environmental variability among the 10 sampling stations (Fig. 2a). The first axis (40.7%) established a horizontal spatial gradient across the eddy (east-core-west) (Fig. 2a), with stations 2 and 5 (eastern edge) and stations 24 and 27 station (western edge) showing the highest dissimilarity and highest contribution to sample variance (Supplementary Table S3). This variance was mainly driven by NH_4^+, temperature, SiO_4^{4-} or deep chlorophyll maximum depth (DCM) (Supplementary Table S3). The second axis (21.2%) distinguished the core stations (15 and 18) that contain water more preserved over time, from the frontal systems containing newly integrated waters at the edges and periphery stations (Fig. 2a). This distinction was mainly driven by PO_4, pycnocline depth, oxygen and NO_2^- (Supplementary Table S3). The potential interplay between these environmental parameters suggests the possibility of distinct habitats for coexisting microbial populations within the eddy.

Measured particulate organic carbon (POC) and nitrogen (PON) showed variations among particles with different sinking rates, collected as fractions ('suspended', 'slow-sinking' and 'fast-sinking') with a marine snow catcher (MSC; see Methods). Considering the sampling volumes from each fraction and assuming all particles were initially homogenised throughout fractions, at the time of bottle closure there was 45% of total particulate organic matter in the suspended, 45% in the slow-sinking, and 10% in the fast-sinking fraction. After settling on deck for 5 h, there was 38.5% remaining at the top (−7.5%), 35.2% middle (−9.8%), and 26% bottom (+16%), with the highest concentrations observed in the fast-sinking fraction (Fig. 2b). However, the C:N ratio was higher in the suspended fraction as compared to the fast-sinking fraction along the eastern frontal edge of the eddy. Towards the eddy core and the western edge, these ratios became more similar (Fig. 2b). The significantly elevated POC concentrations observed at station 2 are likely attributed to the sampling of a more productive water mass closer to the eastern upwelling[24]. However, this variation does not align with the measured PON concentrations, which remain nearly constant throughout the sampling transect. At stations 2–5 on the eastern front is where a peak of inorganic nitrogen compounds was measured (Supplementary Fig. S1), likely favouring communities better adapted to consume fixed inorganic nitrogen under high-carbon conditions[4,27].

Diazotroph community distribution

The diazotroph community composition identified using the *nifH* marker gene revealed a horizontal spatial gradient shift across samples (Fig. 3a;

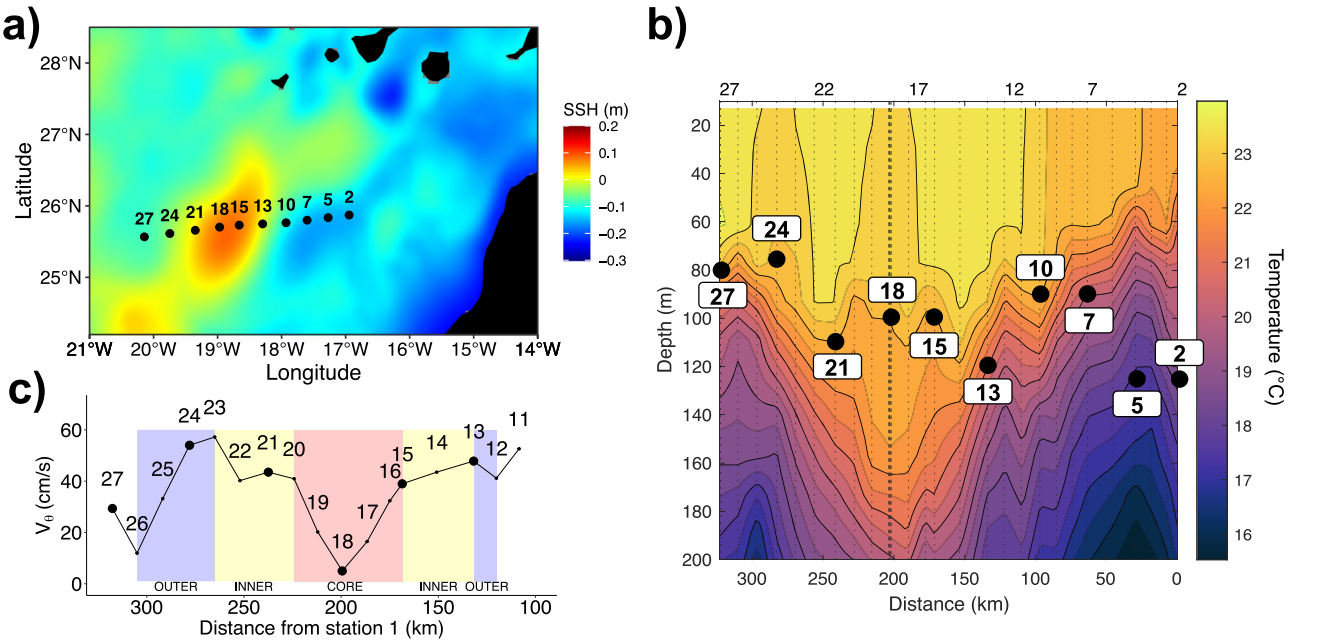

Fig. 1 | Eddy characteristics and sampling stations. a Sampling stations with a marine snow catcher across the anticyclonic eddy "Bentayga" in the Canary Eddy Corridor. The background colour shows the satellite-derived sea surface height (SSH, m), please refer to source data underlying the figure(s) in the data availability statement. **b** Station sampling depths over an interpolated temperature (°C) and depth (m) profile across the eddy. Vertical dashed lines show the hydrographic stations S2–S27, shown in the upper axis every 5 stations. Highlighted the 10 sampling stations for this study. The thick dashed line is the station at the centre of the Eddy (18). The x-axis shows the distance (km) of the sampling transect traversing the Eddy in diagonal. **c** Substructure of the eddy and sampling stations. The substructure is based on the current velocity perpendicular to the transect (absolute value of azimuthal velocity) obtained with the SADCP at 50 m. The centre of the anticyclonic eddy is observed at station 18, within the core (stations 15–20, red background), surrounded by an inner ring (stations 13–15 and 20–23, yellow background) and an outer ring (stations 12–13 and 23–26, blue background). The stations outside the main structure (stations 2–11 and 27, white background) are considered periphery. The sampling stations for this study are highlighted with big bold points.

Supplementary Fig. S2), mainly explained by temperature, C concentration, C:N ratio and the integrated east-west velocity (5.8%, 2.3%, 2.3% and 2% respectively; Supplementary Fig. S3). Similar to the variance seen in the physicochemical parameters (Fig. 2a), the two eastern and two westernmost stations on the periphery of the eddy were positioned at opposite sides of the plot, with the rest of the stations falling in between (Fig. 3a; Supplementary Fig. S4). This supports previous research on eddies, indicating that stirring and trapping can influence microbial communities zonally beyond their vertical pumping effects[28].

Alpha diversity analyses revealed no significant differences among MSC fractions (Kruskal–Wallis, $p = 0.082$; Supplementary Table S4). However, a significant distinction emerged between the slow and fast-sinking fractions in one-to-one comparisons (Wilcoxon, $p < 0.05$, Supplementary Table S5). This significant difference could be related to a particular parameter, such as the differences in particulate organic matter concentrations (Fig. 2b). The type of organic matter composition may therefore play a key role attracting different communities in the slow and fast-sinking fractions. Horizontally, there was a clear significant difference on the diazotroph diversity seen at station and substructure level (Kruskal–Wallis, $p < 0.05$; Supplementary Table S4). The Shannon diversity decreased gradually from east to west (Supplementary Fig. S5; Supplementary Table S6), aligning with previous observations of unique communities in frontal regions[29]. Station 21 presented exceptionally high mean diversity (Kruskal–Wallis, $p < 0.05$; Supplementary Fig. S5a) significantly different to western and central stations (Supplementary Table S7) and within its substructure (Supplementary Table S8), despite physicochemical similarities with these neighbouring stations (Fig. 2a). This is likely influenced by microscale environmental factors (substrate composition) and biotic features (e.g., grazing, colonisation dynamics) not considered in this study, and maybe attributed to water mixing with the west filament and the downwelling pumping near the core[30]. Similar to Alpha diversity, Beta diversity analyses revealed significant diazotroph community variations across the eddy (Adonis PERMANOVA, ANOSIM, $p < 0.05$; Supplementary Table S9), primarily driven by the stations (61.24% contribution; Kruskal–Wallis, $p < 0.05$), while MSC fractions made a minor contribution (4.49%) with no significant differences between them (Adonis $p = 0.06$; ANOSIM $p = 0.7$; Supplementary Table S9).

Variations in diazotroph community composition among stations may result from different adaptations to the physicochemical heterogeneity, including their energy acquisition strategies, whether they are cyanobacteria or NCDs. Overall, 52% of the total reads were annotated as cyanobacteria (Fig. 3b), dominating the suspended (60% reads; 80% samples; Supplementary Data 1) and the slow-sinking fractions (53.9% reads; 70% samples), but not the fast-sinking fraction (41.6% reads; 50% samples) where NCDs were more abundant (58.4% reads; 50% samples). Stations 2 and 21, were entirely dominated (>50% reads) by NCDs in all fractions, whereas stations 7, 10, 15, 24, and 27 were dominated by Cyanobacteria (Fig. 3b). Both groups were found in all stations and all fractions, which is not rare given the wide physiological diversity within each group[4]. However, while there was a lack of significant differences in the distribution of cyanobacteria and NCDs across sample groups (Wilcox, p-value > 0.05), the highest percentage of NCD abundance on each station was always found in the fast-sinking fraction (except station 2) compared to the upper fractions (Supplementary Data 1). This may suggest that most of the NCDs were associated with fast-sinking particles, while cyanobacterial diazotrophs were more prevalent in the suspended or slow-sinking with smaller particles containing less carbon (Fig. 2b).

Cyanobacteria. UCYN-A (recently reconsidered as the nitroplast organelle[31,32] was prevalent and ubiquitous in all samples, accounting for an average of 48.6 ± 22.9% *nifH* reads per sample (Supplementary Data 1). Within the cyanobacteria, UCYN-A was the predominant group (Fig. 4b; Supplementary Data 1), commonly found in anticyclonic eddies in the North Pacific with up to 10^6 *nifH* gene copies L^{-1}[33], but not in

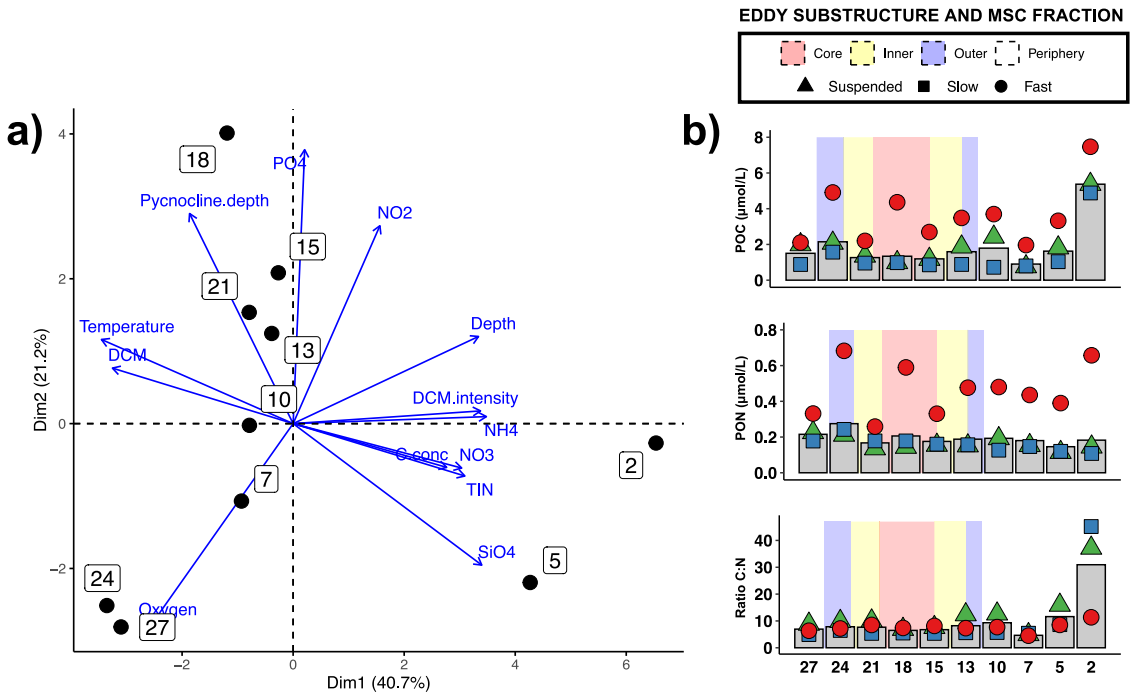

Fig. 2 | Environmental variability across stations. a Biplot based on a principal component analysis (PCA) showing the variability across the 10 sampling stations using the physicochemical parameters. Blue arrows represent the top parameters indicate the direction and magnitude of the variables' contribution to the principal components. Variables include: temperature, oxygen, sampling depth, deep chlorophyll maximum (DCM chlorophyll value in mg/m^3), DCM intensity (chlorophyll difference between surface and DCM), pycnocline depth (based on temperature and salinity with a density gradient threshold value of 0.04), bottle averaged particulate organic carbon (C. concentration), and nutrients: nitrate (NO_3), nitrite (NO_2), ammonium (NH_4^+), Total Inorganic Nitrogen (TIN), phosphate (PO_4^{3-}) and silicate (SiO_4^{4-}). **b** Measured concentrations of POC, PON (µmol/L), and C:N ratio in the MSC for each sampling station. MSC fractions are differentiated by colour and shape. Grey bars represent the average value of the three MSC fractions for each parameter. Background colour represents the eddy substructure characterised with azimuthal velocities: core (red), inner ring (yellow), outer ring (blue) and periphery (white).

cyclonic eddies[16,17,34]. An exception occurred in the suspended particle fraction at station 5, where *Crocosphaera* dominated instead (Fig. 4a, b; Supplementary Data 1; 58% overall reads), becoming the second most abundant cyanobacterial group of the dataset. While *Crocosphaera* is typically low or unreported in the northeast compared to the southwest Atlantic[35,36], high abundances have been linked to high N_2 fixation rates measured in anticyclonic eddies in the North Pacific[19,33]. In this study, 99% of the *Crocosphaera* sequences were found between stations 2 and 7, seemingly forming a bloom at the eastern edge of the eddy. Given the sporadic occurrence of this group, it is likely that the appearance of *Crocosphaera* is attributed to either the physical accumulation at the eastern front between water bodies or to a response to a new nutrient input[33]. The third most abundant cyanobacterium was *Trichodesmium*, found in 19 out of the 30 of the samples (Fig. 4a, b). While *Trichodesmium* usually thrives in warm waters[37], its distribution here was primarily concentrated along the cold-water eastern edge of the eddy (stations 2–7 comprised 78% of *Trichodesmium* reads; Supplementary Data 1), and present in the western edge, but absent in the core and western inner ring (stations 15–21; Fig. 4a). Various hypotheses are considered to explain accumulations of this cyanobacterium in response to eddy-wind interactions[38,39], local nutrient inputs, or advection and trapping from areas where communities are more abundant[40]. In anticyclonic eddies in the North Atlantic, high *Trichodesmium* abundances are commonly observed[41,42], particularly at the edges with submesoscale upwelling inputs, which could serve as a nutrient source[43]. Therefore, the prevalence of *Trichodesmium* was predominantly driven by the physical accumulation at the frontal systems at the outskirts of the eddy where density contrasts exist[39,44], specifically in this region[45] rather than by temperature.

UCYN-A and *Trichodesmium* were indistinctively detected in all MSC fractions, reflecting their vertical movement capabilities. This is not rare since while *Trichodesmium* uses gravitational sinking and buoyancy mechanisms[46–48], UCYN-A, being a symbiotic organism, benefits from host ballasting and associations with calcium carbonate hosts[49], contributing significantly to carbon export[8].

Non-cyanobacterial diazotrophs. NCDs accounted for the remaining 48% of *nifH* reads (Fig. 3b; Supplementary Data 1), emphasising that in dynamic systems like anticyclonic eddies, these can be as abundant and potentially as active, as cyanobacterial diazotrophs. Their prevalence in eddies has been explained by organic matter accumulating at the core of anticyclonic eddies[18] or alleviation of phosphorus stress in cyclonic eddies[50]. Overall, Gammaproteobacteria (mostly *Marinobacter*) was the most abundant NCD group (16.9 ± 11% of *nifH* reads) across the eddy, followed by Betaproteobacteria (14.9 ± 8%) and Alphaproteobacteria (7 ± 5%). The wide biogeography and depth range of Gammaproteobacteria has been explained by their capability of associating with different particle sizes[8,11]. While Alphaproteobacteria and minor NCD groups were predominant in only 3 and 2 samples out of 30 respectively, Betaproteobacteria (in 13 samples) and Gammaproteobacteria (in 12 samples) exhibited similar dominance across samples, indicating significant contributions from both groups to the NCD community dynamics in the studied environment.

Horizontally, in the suspended and slow-sinking fraction Gammaproteobacteria dominated on the east and Betaproteobacteria on the west, while in the fast fraction Gammaproteobacteria dominated in the core and had higher abundance in the east than the west. This was supported by significant differential abundances of these groups between stations from the east (5,7) and the west (21,24,27) (Deseq2, $p < 0.05$; Supplementary Table S10). Alphaproteobacteria was notoriously present, dominating the NCD community in both eddy fronts in the fast-sinking fraction (Fig. 4a, b). Interestingly, Betaproteobacteria showed a statistically significant but

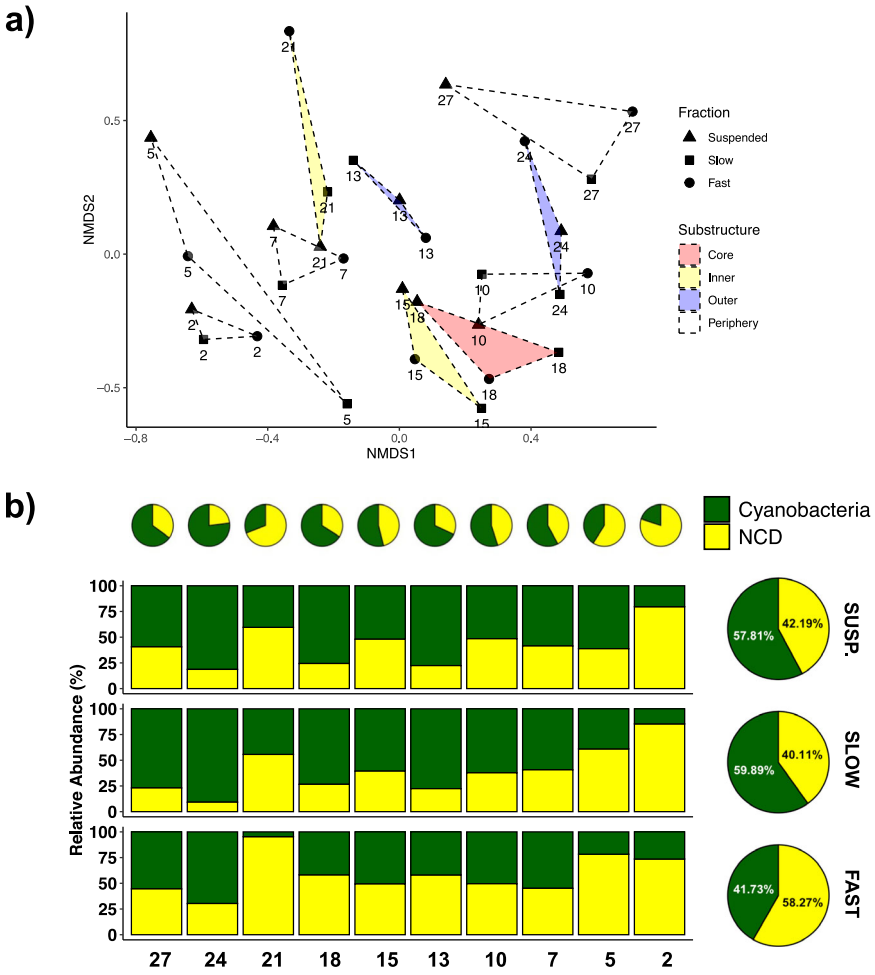

Fig. 3 | Diversity of the diazotroph community across samples. a Non-parametric multi-dimensional scaling (NMDS) based on Bray–Curtis distance considering all nifH sequences from all the samples. Numbers refer to station numbers and point shapes correspond to the three MSC fractions "Suspended", "Slow" and "Fast-sinking". Dashed triangles are drawn joining the three MSC fractions of each station. Triangle colour scale corresponds with eddy substructure characterised with azimuthal velocities: core (red), inner ring (yellow), outer ring (blue) and periphery (white). **b** Relative abundance of the cyanobacteria and non-cyanobacterial diazotrophs (NCDs) based on the nifH amplicon across stations and fractions (left) and averaged abundance across stations per fraction (right).

moderate negative relationship with Gammaproteobacteria (R = −0.47, *p*-value < 0.05, Supplementary Data 2), establishing community niche differentiations across the eddy substructure, This suggests that while Gammaproteobacteria may be more competitive in particle accumulation frontal zones of environments with colder-water and high iron to phosphorus ratios[51,52], close to the African coast, Betaproteobacteria may be more competitive in warmer-waters with residual nutrients at surface. Despite the wide diversity of metabolic lifestyles within Gammaproteobacteria, it is likely that their distribution is driven by the availability of nitrate and phosphate dragged from the eastern front, contrary to Betaproteobacteria which lack nitrate transporters[4].

Alphaproteobacteria (mainly *Hyphomicrobiales*, formerly *Rhizobiales*) dominated exclusively in the fast-sinking fraction, particularly at the eddy edges (stations 2, 24, 27; Fig. 4a, b). Alphaproteobacteria was the only NCD group differentially abundant across fractions specifically between suspended and fast-sinking and slow and fast-sinking (DeSeq2, $p < 0.05$; Supplementary Table S10). Although not typically considered a major player in marine ecosystems, *Hyphomicrobiales* is a metabolically and morphologically heterogeneous group[53]. This group has been documented in studies focused on deep environments, such as hydrothermal vents displaying quorum sensing activities[54], or marine sediments, where it may be involved in organic matter degradation. Genera within *Hyphomicrobiales* include aerobic chemoheterotrophs and facultatively methylotrophs. Some members can grow anaerobically by denitrification or fermentation[55], whereas some terrestrial groups can be photosynthetic[56]. Additionally, Alphaproteobacteria showed a significant negative correlation with UCYN-A (R = −0.43, *p*-value < 0.05, Supplementary Data 2). The slight tendency to decrease in relative abundance when UCYN-A is more prevalent, could be attributed to a habitat preference of UCYN-A near the surface[57] and Alphaproteobacteria in deep environments as explained above, rather than a resource competition.

Two samples from the eastern stations showed an exceptional diversity in community composition. The suspended fraction on station 5 where *Crocosphaera* dominated, was the only station not dominated by Proteobacteria, but by a merged group of other NCDs without annotated taxonomy in the database (Fig. 4). In addition, high relative abundance of *Desulfuromonadia* (previously Deltaproteobacteria[58]), was found in the slow-sinking fraction of the carbon-rich station 2 (67% of NCD reads and 58% overall *nifH* reads; Supplementary Data 1), often seen deeper down the water column or marine sediments[59]). In this station, the highest values of some types of inorganic nitrogen were found (Supplementary Fig. S1), however, as Deltaproteobacteria MAGs have been reported to lack nitrate, nitrite, and urea transporters[4], their high abundance may not be related to nitrogen availability. Instead, *Desulforomonadia* may be favoured in high C:N ratio environments (Fig. 2b), outcompeting other Proteobacterial diazotrophs.

Station 21, characterised by the highest Alpha diversity (Supplementary Fig. S5) and NCD dominance in all fractions (Fig. 3b), was explained by its unique NCD community. Betaproteobacteria accounted for >50% of the overall diazotroph reads in the fast-sinking fraction (Fig. 4b; Supplementary Data 1) with noticeable peaks of the genera *Aquabacterium* or Gammaproteobacteria *Xanthomonadales*.

Environmental drivers influence the diazotroph community structure. The environmental parameters and relative abundances of cyanobacteria and NCD groups were assessed as a proxy to study how the energy-obtaining lifestyle may be key in adapting to the eddy dynamics. Significant positive correlations were observed for

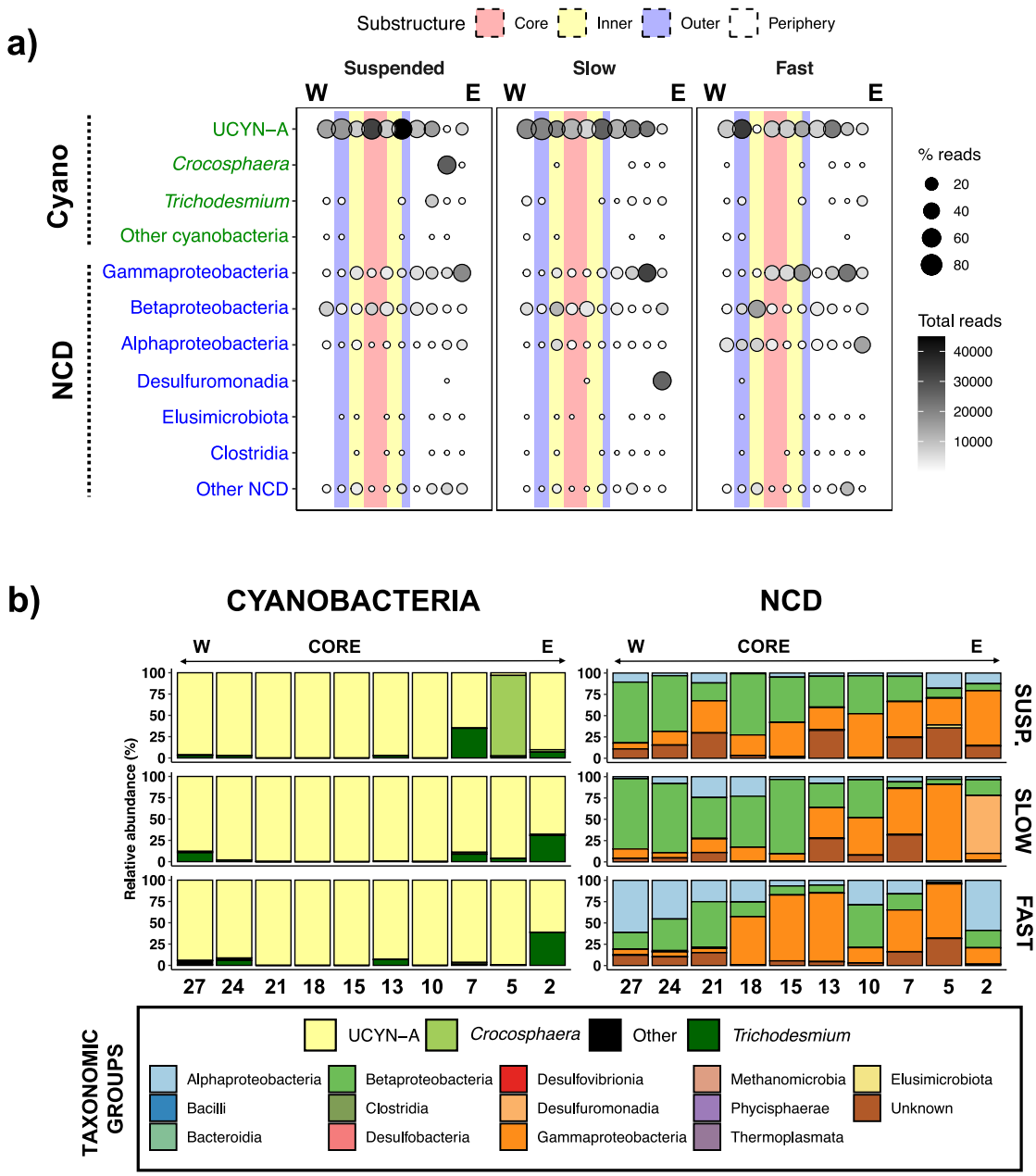

Fig. 4 | Relative abundance of the cyanobacteriaL and non-cyanobacterial diazotrophs based on the nifH amplicon. a Overall relative abundance of all diazotrophs across fractions (Suspended, Slow and Fast) and samples (horizontal). Bubble size corresponds to the percentage of read counts per taxa. "Other" cyanobacteria and NCDs include unknown taxa and groups with <1% average reads in the dataset such as Desulfovibrionia, Phycisphaerae, Bacilli, Desulfobacteria, Thermoplasmata, Methanomicrobia, Bacteroidia. Background colour represents the eddy substructure characterised with azimuthal velocities: core (red), inner ring (yellow), outer ring (blue) and periphery (white). **b** Relative abundance for individual groups within Cyanobacteria genus (left) and NCD class (right).

cyanobacteria with UCYN-A (R = 0.87, as is the dominant phylotype), PON, temperature, dissolved oxygen, DCM depth and salinity (R = 0.73, 0.61, 0.53, 0.52, 0.41, respectively); whereas NCDs were correlated with Alpha diversity indices, depth, C:N ratio of particulate organic matter, DCM intensity, longitude, POC per fraction and Gammaproteobacteria (R = 0.76, 0.71, 0.67, 0.60, 0.55, 0.53, 0.50, respectively) (Fig. 5; Supplementary Data 2). It is worth noting that when working with relative abundances, the complementary nature of the two phylogenetic groups yields an inverse abundance relationship; as one increases, the other decreases. Likewise, parameter correlations within each group show opposing trends, while one group exhibits positive correlations with a group of parameters, the exact values but in negative will be found for the other group.

Diazotroph heterogeneity primarily resulted from NCD diversity, evidenced by significant correlations with diversity indices (Fig. 5). Autotrophic groups may have lower diversity given the evolutionary biochemical challenge integrating oxygenic photosynthesis and N_2 fixation (reviewed in ref. 60). The strong positive correlation with PON, temperature and dissolved oxygen hints cyanobacteria (mainly UCYN-A) might be the main contributor to N_2 fixation in the anticyclonic eddy "*Bentayga*", enhanced by temperature and dissolved oxygen, although additional measurements or transcriptional analysis are needed to confirm it. The capability of UCYN-A to fix N_2 aerobically is not uncommon, as it uses host photosynthesis[61] and hopanoid-enriched membranes to overcome the inhibition of the N_2 fixation enzyme by oxygen[62]. Since this study aimed at elucidating diazotroph community structure differences among particle fractions, N_2 fixation rate

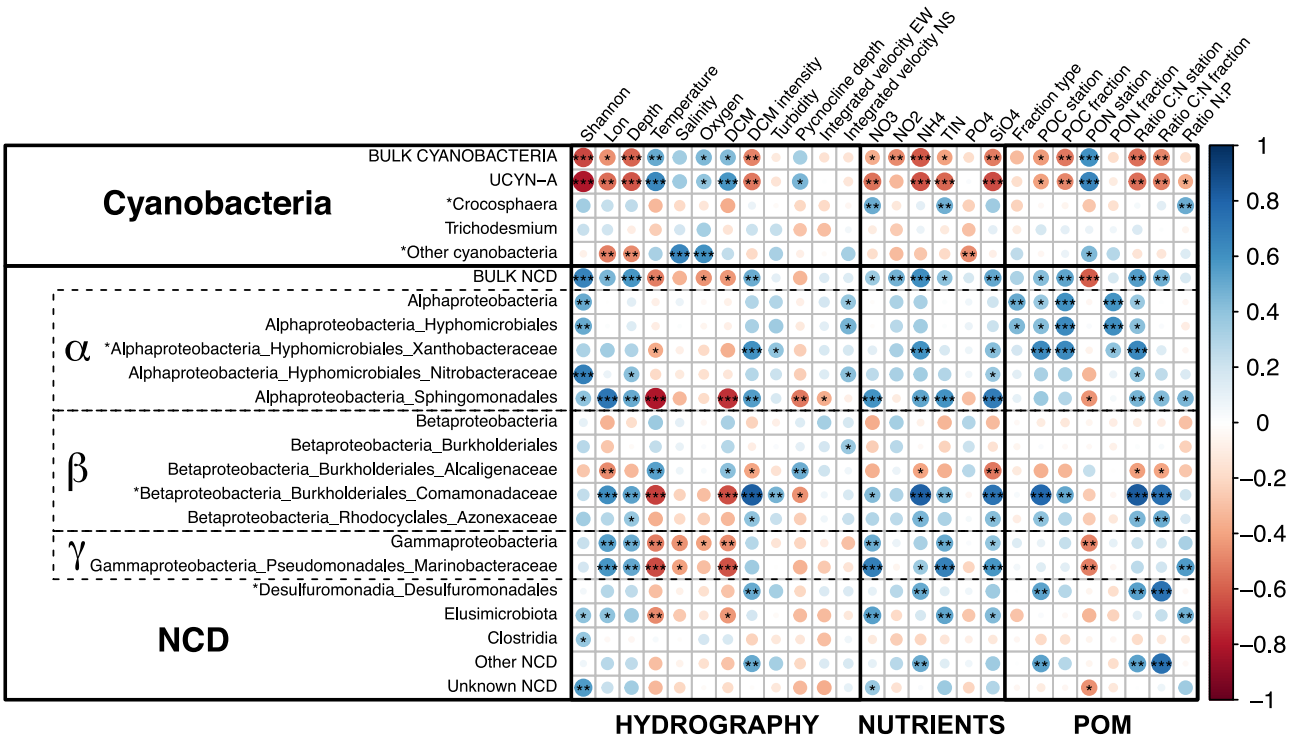

Fig. 5 | Correlation between environmental parameters and relative abundances of top diazotroph groups ($n = 30$) including: bulk cyanobacteria and NCDs, and individual phylotypes form each group (genus level for cyanobacteria and order level for NCDs). Individual phylotypes shown are the most abundant phylotypes and those who show significant correlations. Taxonomic groups labelled with (*) are found in <50% of the samples and caution needs to be applied when interpreting results. Parameters include diversity index Shannon and measured environmental variables. Hydrography: longitude, sampling depth, temperature, salinity, dissolved oxygen, DCM depth, DCM intensity, turbidity, pycnocline depth, integrated velocities east-west and north-south. Nutrients (μmol/L): NO_3^-, NO_2^-, NH_4^+, Total Inorganic Nitrogen (TIN), HPO_4^{2-}, H_4SiO_4. Particulate Organic Matter (POM): fraction type, POC, PON, C:N ratio, and N:P ratio. Some values are specified as of station (averaged MSC bottle) and fraction (individual sinking fractions). Colour scale indicates the Pearson correlation test coefficient form positive (blue) to negative (red). Significance levels are shown as: ***<0.001, **<0.01, *<0.05, blank = non-significant.

or quantitative gene abundance measurements were not considered. Therefore, it cannot be conclusively determined whether cyanobacterial groups or particle-associated NCDs[63] were the primary contributors of nitrogen fixation in this eddy.

Deeper layers with higher sinking-carbon accumulation, where light is scarce, support organic matter dependent communities. No direct correlation was found between NCDs and water turbidity. However, this parameter encompasses diverse optical properties beyond just organic matter presence, making it an imprecise measure for linking NCDs to organic matter. The significant positive correlation with the POC as well as with the C:N ratio aligns with knowledge from marine aggregates, characterised by high C:N ratio values and high availability of labile carbon supporting their high energy requirements[13].

No significant correlations were found between *Trichodesmium*, and the environmental parameters considered (Fig. 5; Supplementary Data 2), supporting the frontal "passive" accumulation hypothesis. This suggests physical accumulation by fine-scale dynamics at the peripheric stations (Fig. 4b) rather than active involvement in N_2 fixation activity[39,44]. Exceptionally, a correlation was found between *Crocosphaera* and NO_3, and consequentially with TIN and the N:P ratio (Fig. 5; R = 0.50, 0.49, 0.50). While the physical accumulation at the eastern edge may have also affected *Crocosphaera*, their proliferation at a single station was likely directly related to the peak in NO_3 seen in station 5, where NH_4^+ was also high (Supplementary Fig. S1), since *Crocosphaera* can be a major consumer of fixed nitrogen[64]. This would be consistent with other studies that directly link peaks in measured nutrient concentrations with high abundances of diazotrophs or elevated nitrogen fixation rates[1,65,66]. UCYN-A, however, showed similar correlations to that of the overall cyanobacterial relative abundance, as it was the dominant group (Fig. 5). Positive correlations were found with PON, temperature and DCM (R = 0.65, 0.65, 0.58), and negative with depth, C:N ratio, longitude, DCM intensity, POC (R = −0.62, −0.56, −0.55, −0.53, −0.48). Lastly, the unknown group of cyanobacteria was positively associated with salinity and dissolved oxygen (R = 0.65, 0.61).

Within the NCD groups, Gammaproteobacteria showed positive correlations with longitude, overall NCD relative abundance and depth (R = 0.54, 0.50, 0.49), and negative correlations with temperature, bottle PON and DCM (R = −0.55, −0.48, −0.46). The negative correlation of Gammaproteobacteria with temperature contradicts global trends observed[4]. However, as this is a subtropical region with a gradual temperature range spanning only 5 °C, it is likely this correlation was not causal and could be due to the mixing of the eastern frontal system. The distribution of Alphaproteobacteria was the only group influenced by the type of sampled fraction, displaying positive correlations with fraction type as well as with measured POC and PON in those specific fractions (R = 0.60, 0.60, 0.50). This was supported by the significant increase in relative abundance in the fast-sinking fraction compared to both the slow and suspended fractions (Deseq2, p value < 0.05; Supplementary Table S10). Given the observation that Alphaproteobacteria were primarily abundant in the fast-sinking fraction in this study, the positive correlation between POC and PON within this fraction suggests that out of the NCDs, this group likely plays a significant role in contributing sinking particulate organic matter. Interestingly, bulk Betaproteobacteria did not show correlations with any environmental parameter, whereas certain subgroups within the *Burkholderiales* order did (Fig. 5). Due to limited available data on Betaproteobacteria[4,7], it could be speculated that Betaproteobacteria niche differentiation across the eddy is influenced by the metabolic potential of these unexplored subgroups. For instance, the family *Burkholderials Comamodaceae* seems metabolically more similar to Gammaproteobacteria

contrasting with *Burkholderiales Alcaligenaceae* (Fig. 5). Other minor NCD groups had strong correlations with the C:N ratio per fraction and total POC per bottle (R = 0.74, 0.55), confirming a direct relationship with carbon resources in line with their energy requirements.

Overall, measured nitrogen, silicate and phosphate nutrients showed positive significant correlations with some individual NCD subgroups, and negative correlations with UCYN-A (Fig. 5). The presence of inorganic nitrogen does not necessarily limit N_2 fixation[67], and can be beneficial for NCDs[68,69]. Therefore, high inorganic nitrogen (NO_3^-, NH_4^+ and TIN) and high C:N ratio of particulate organic matter from the eastern filament at stations 2–5 may have favoured the dominance of the NCD community.

Discussion

Horizontal advection shapes diazotroph community over sinking speeds

The patchiness of distribution observed across the eddy is the result of various sub-mesoscale processes, such as horizontal stirring and biotic interactions[70]. In this anticyclonic eddy, the pronounced impact on diazotroph diversity was primarily attributed to the two main frontal zones. These zones displayed higher rotational velocities at the peripheries compared to the core (Fig. 1c), creating a strong horizontal signal (Fig. 3a) and leading to fine-scale patterns of significant niche differentiation among diazotrophs between the west and the east of the transect (Supplementary Table S10).

While the environmental and biogeochemical conditions of station 21 were similar to the neighbouring stations (Fig. 2a), a distinct diazotroph community was observed (Fig. 3a). This station was dominated by NCDs, notably in the fast sinking fraction where Betaproteobacteria groups made up 51.1% of the total *nifH* reads (Supplementary Data 1). Since the biogeochemical variables did not explain such differences, it can be speculated that this may be due instead to competition in particle space or due to enhanced vertical flux of particles at this close-to-centre station, transporting particles and associated communities faster into deeper layers[71] than with gravitational sinking alone[72]. Notably, station 21 had the lowest DCM intensity and the second-deepest DCM, indicating the potential sinking of organic carbon, serving as an energy source for heterotrophic communities. Here, a passive process driven by rapid stirring, outpaced the in situ biological rates of change (e.g., vertical sinking) and ecosystem processes shifting community structure[73]. This raises new questions regarding the significance of mesoscale eddy dynamics in influencing diazotroph diversity rather than their productivity. Future studies will need to investigate to what extent the horizontal swirling and vertical mixing of water masses propagate throughout the water column affecting the contribution of both particles and the attached NCD community down to the bathypelagic layer[74].

Particle type hints key contributors to nitrogen and carbon cycling

The composition, porosity and density of particles are determinants of unique biogeochemical conditions within individual structures, offering distinct ecological niches for specialised taxonomic groups[10]. Although the presence of NCDs in individual particles is highly variable[10], it is key to establish a differentiation between the type of particles. However, since components of organic matter were measured in bulk, and not all groups were uniformly present across fractions or stations, it is necessary to look beyond overall correlations. Differences in POC and PON among fractions (Fig. 2b) established particle compositional differences between suspended and sinking fractions, creating unique microenvironments which favoured the association of specific groups. This ecological niche partitioning at sinking-fraction level was only seen for NCD groups, such as high overall Alphaproteobacteria abundance in fast-sinking fractions driven by order *Hyphomicrobiales*, or the specific Alphaproteobacterial genus *Bradyrhizobium* predominant in suspended and slow-sinking fractions. This genus is often found in diazotroph studies, sometimes dominating the diazotrophic populations such as in the Mediterranean Sea[75]. Interestingly, certain terrestrial *Bradyrhizobium* are capable of photosynthesis[56], requiring light for energy production. As this group dominated only in the upper-fractions, their potential for photosynthesis in the marine environment should not be overlooked. These differences underline their capacity to use specialised physiological strategies adapted to thrive in a variety of anaerobic and carbon-rich environments (suspended, slow and fast-sinking particles)[13]. Additionally, NCDs appeared to be more abundant in the eastern periphery (Fig. 3b) where conditions of excess carbon were observed (Fig. 2b). This was evident in the higher C:N ratio of particles (Fig. 2b), indicating the presence of more refractory carbon-related material which is harder to degrade[76]. Stations 2–5 at the periphery exhibited biological similarities, contrasting with stations 24–27 (Fig. 3a), which contained distinct organic matter compounds (Fig. 2b). It could be considered then that the different communities associated with different type of particles on the east and west of this transect could play distinct roles in export. However, it is important to note that quantitative data would be needed to draw firm conclusions.

Here, sedimentation time was set as a density differentiation parameter to separate types of particles. As the gravitational settling of particles is a major mechanism for carbon export into deep waters, the sinking velocity can provide insight into the particle behaviour. In fact, the efficiency of the biological carbon pump depends on the amount of organic matter exported and the remineralisation rate (breakdown and respiration of sinking organic matter[77];). For this reason, fast-sinking particles are expected to be the main contributors to the deep ocean compared to slow-sinking particles that are rapidly recycled in shallower depths[8]. Specifically, sinking velocity depends on several particle factors, including size, shape, porosity and mass, as well as water properties such as viscosity. Particle size and composition are critical parameters in understanding the sinking velocity, the amount of organic material and organism specificity[78–80]. Although the spectrum of particle velocities is wider, the study of carbon export from sinking particles could be simplified into three fractions, such as done in this study. Based on the distance between taps (65 cm) and the incubation time (4–5 h) of this study, the sinking velocity of each fraction was estimated to be: <1.5 m d^{-1}, ~3 m d^{-1} and >3 m d^{-1} for the suspended, slow-sinking, and fast-sinking particle fractions, respectively. However, observations from global particulate organic matter flux datasets suggest >85% of the flux can be explained in a bimodal distribution on <10 and >350 m d^{-1} [81]. By applying these thresholds, the suspended and slow-sinking fractions here would contribute differently than most -but not all- of the fast-sinking fractions, explaining some community differences seen. However, no accurate measurements were done to measure individual sinking velocities, and the velocity ranges would depend again on the particle type (mostly density), for example from aggregates with cyanobacteria in the laboratory 100–400 m d^{-1} [82], or diatom aggregates of plankton faecal pellet 5–732 m d^{-1} [79].

Understanding the ecology of particle-associated diazotrophs within eddies is essential, as it complements the current knowledge of horizontal and vertical (sinking) flux dynamics in these environments. Given the potential important role of NCDs in carbon export and nitrogen supply into marine ecosystems, and the anticipated increase in frequency and intensity of eddies in the next decades[83], this work offers valuable insights into the mechanisms controlling diazotrophy in the context of mesoscale structures. For this, future research is needed to understand the mechanisms driving particle aggregation of diazotrophs, and their associated sinking and recycling speeds to enhance the existing carbon export models.

Materials and methods

Eddy characterisation and sample collection

This study was conducted onboard the B/O *Sarmiento de Gamboa* during the e-IMPACT2 cruise (November 7th to December 7th, 2022) south of the Canary Islands in the Northeast Atlantic (Fig. 1). The anticyclonic eddy named "*Bentayga*" was localised using satellite altimeter data, including sea level anomalies and derived geostrophic currents (available at https://www.aviso.altimetry.fr). A total of 26 hydrographic stations were surveyed along a section, spaced approximately every 5 km, with only 10 stations sampled for diazotrophs (Fig. 1; Supplementary Table S11). The physical environment of the eddy was characterised using shipboard acoustic Doppler current profiler (SADCP) measurements from a 75 kHz RDI Ocean Surveyor. The

SADCP provided mean current profiles relative to the ship in 16-metre bins using the narrow-band profiling mode. Data were processed with CODAS software (https://currents.soest.hawaii.edu/docs/adcp_doc/) and averaged over time at each station, as described by Martínez-Marrero et al.[84]. The substructure of the eddy (core, inner and outer rings, and periphery) was determined using the data on the velocity perpendicular to the transect (azimuthal velocity) obtained with the SADCP. Hydrographic data were measured using a conductivity-temperature-depth (CTD) probe (SeaBird SBE911 plus), along with sensors for dissolved oxygen (SeaBird SBE43), fluorescence of chlorophyll (SeaPoint SCF), and turbidity (SeaPoint STM).

To collect sinking particles, a marine snow catcher (MSC, OSIL, UK) was used at 10 stations (Fig. 1). Deployed at 10 m below the deep chlorophyll maximum depth (DCM, 80–120 m; Supplementary Table S11) as in Fadeev et al.[85], the MSC was recovered and settled for 5 h before gentle emptying (~1–1.5 L min^{-1}) to avoid turbulence. Three fractions based on material sinking speed: "suspended", "slow-sinking" and "fast-sinking", (38 L, 38 L and 9 L respectively) were separated for particulate organic matter and amplicon sequencing.

Chemical analyses

Particulate organic matter (POC and PON) from the three fractions of the MSC was collected in 25 mm pre-combusted (450 °C, 4 h) GF/F filters under gentle vacuum, dried overnight in a vacuum desiccator with silica gel and frozen at −20 °C until determination in the base laboratory. The filters were analysed in a CHN elemental analyser Perkin Elmer 2400 CHN as in Valiente et al.[86]. Filtered volumes were 5 L for the 'suspended' and 'slow-sinking' fractions and 3 L for the 'fast-sinking' fraction.

Nutrient salts (nitrate, nitrite, ammonium, phosphate, and silicate) concentrations in the water column were determined simultaneously by segmented flow analysis in an Alliance Futura autoanalyser following the methods of Hansen and Koroleff[87] except for the case of ammonium, which was measured by the fluorometric method of Kerouel and Aminot[88] (Supplementary Table S2). To obtain the nutrient values at MSC sampling depths, values were interpolated based on temperatures using the water column profile.

Biological sampling, DNA extraction and *nifH* gene amplification

The 'suspended' (20 L), 'slow-sinking' (20 L) and 'fast-sinking' (3 L) fractions of each MSC was filtered through 25 mm 0.2 µm Supor® filters (hydrophilic polyethersulfone) using a Masterflex L/S peristaltic pump (Cole-Palmer, Illinois, USA). Filters were placed in previously autoclaved bead-beater tubes containing 0.1 and 0.5 mm microbeads, frozen in liquid nitrogen, and stored at −80 °C. Thirty DNA samples were analysed for this study (3 fractions from 10 stations). An additional sampling station outside the eddy termed "outfield" (1 MSC, 3 fractions) was analysed to compare the diversity on the area outside the eddy (Supplementary information). Extraction of the nucleic acids was performed using the DNeasy Plant Mini Kit (Qiagen, Manchester, UK) following the protocol of the manufacturer with minor modifications as in Bonnet et al.[8]. Nested (two round) polymerase chain reaction (PCR) was used to amplify the *nifH* genes using degenerate primers, and second round primers nifH1 and nifH2[89]. Partial Illumina adaptors were used in the second round for the Genewiz sequencing facility (Leipzig, Germany). Reagent mix and protocol was done as in Bonnet et al.[8], (Supplementary Information). Triplicate amplifications of samples were pooled to maximise gene detection. PCR products were run on 1.5% agarose gels, extracted and purified with Wizard SV Gel and PCR Clean-Up System (Promega, Wisconsin, USA), and eluted in 30 µL.

Sequence quality control and taxonomic assignment

nifH amplicons were successfully amplified from all samples. Pre-processing and normalisation of raw data was done in R (4.2.2) using the DADA2 pipeline[90]. On average, 66,884 reads per sample were retrieved (ranging from 59,670 to 79,219; Supplementary Table S12), resulting in 9522 amplicon sequence variants (ASV). Taxonomic ranks for the *nifH* diversity were assigned based on the database M. A. Moynihan & C. Furbo Reeder 2023. (nifHdada2 GitHub repository, v2.0.5. Zenodo; https://doi.org/10.5281/zenodo.7996213). This resulted in 1587 unique ASV, 77 for Cyanobacteria phylum, and 1510 for non-cyanobacterial groups (Supplementary Table S13).

Statistical analyses

The dataset was analysed in R (v 4.3.1) using *phyloseq* 1.45.0[91], *vegan* 2.6.4[92], *microbiome* 1.23.0[93] and visualised with *ggplot2* 3.4.3. Alpha diversity analysis was assessed using Shannon and Simpson indices and Kruskal–Wallis[94] and Wilcoxon[95] tests to determine the effect of sample types on diazotrophs. Beta diversity analysis was assessed through a permutational multivariate analysis of variance (Adonis), and analysis of dissimilarity (ANOSIM) based on Bray–Curtis distances to test the community differences between sample groups. The significance level for both analyses was set at $p < 0.05$. Differential abundance analysis was done using DeSeq2 1.42.0[96] with an adjusted p-value < 0.05 calculated using Benjamini–Hochberg correction. Correlations between environmental variables and relative abundances were performed with *corrplot*, using a Person parametric correlation test ($p < 0.05$).

Reporting summary

Further information on research design is available in the Nature Portfolio Reporting Summary linked to this article.

Data availability

The background colour in Fig. 1a shows the satellite-derived sea surface height (SSH, m) from 21/11/2022 (Global Ocean Biogeochemistry Analysis and Forecast, L4, E.U. Copernicus Marine Service Information CMEMS DOI: 10.48670/moi-00015). Source data underlying Fig. 2b can be found in Supplementary Table S2 in Supplementary Information. Raw sequences of the amplicon sequencing analysis have been deposited in NCBI as a BioProject accession number PRJNA1039751. The physicochemical data from the co-authors that support the findings of this study are available from the corresponding author upon request.

Received: 13 February 2024; Accepted: 11 July 2024;
Published online: 02 August 2024

References

1. Moore, C. M. et al. Processes and patterns of oceanic nutrient limitation. *Nat. Geosci.* **6**, 701–710 (2013).
2. Zehr, J. P. Nitrogen fixation by Marine Cyanobacteria. *Trends Microbiol.* **19**, 162–173 (2011).
3. Bombar, D., Paerl, R. W. & Riemann, L. Marine non-cyanobacterial diazotrophs: Moving beyond molecular detection. *Trends Microbiol.* **24**, 916–927 (2016).
4. Turk-Kubo, K. A. et al. Non-cyanobacterial diazotrophs: Global diversity, distribution, ecophysiology, and activity in Marine Waters. *FEMS Microbiol. Rev.* **47**, fuac046 (2022).
5. Zehr, J. P., Jenkins, B. D., Short, S. M. & Steward, G. F. Nitrogenase gene diversity and Microbial Community Structure: A cross-system comparison. *Environ. Microbiol.* **5**, 539–554 (2003).
6. Halm, H. et al. Heterotrophic organisms dominate nitrogen fixation in the South Pacific Gyre. *ISME J.* **6**, 1238–1249 (2011).
7. Delmont, T. O. et al. Correction to: Heterotrophic bacterial diazotrophs are more abundant than their cyanobacterial counterparts in metagenomes covering most of the Sunlit Ocean. *ISME J.* **16**, 1203–1203 (2022).
8. Bonnet, S. et al. Diazotrophs are overlooked contributors to carbon and nitrogen export to the Deep Ocean. *ISME J.* **17**, 47–58 (2023).
9. Sohm, J. A., Edwards, B. R., Wilson, B. G. & Webb, E. A. Constitutive extracellular polysaccharide (EPS) production by specific isolates of Crocosphaera Watsonii. *Front. Microbiol.* **2**, 229 (2011).
10. Farnelid, H. et al. Diverse diazotrophs are present on sinking particles in the North Pacific Subtropical Gyre. *ISME J.* **13**, 170–182 (2018).

11. Cornejo-Castillo, F. M. & Zehr, J. P. Intriguing size distribution of the uncultured and globally widespread marine non-cyanobacterial diazotroph gamma-A. *ISME J.* **15**, 124–128 (2021).
12. Pedersen, J. N., Bombar, D., Paerl, R. W. & Riemann, L. Diazotrophs and N2-fixation associated with particles in coastal estuarine waters. *Front. Microbiol.* **9**, 2759 (2018).
13. Riemann, L. et al. Planktonic aggregates as hotspots for heterotrophic Diazotrophy: The plot thickens. *Front. Microbiol.* **13**, 875050 (2022).
14. Chakraborty, S. et al. Quantifying nitrogen fixation by heterotrophic bacteria in sinking marine particles. *Nat. Commun.* **12**, 4085 (2021).
15. McGillicuddy, D. J. et al. Influence of mesoscale eddies on new production in the Sargasso Sea. *Nature* **394**, 263–266 (1998).
16. Fong, A. A. et al. Nitrogen fixation in an anticyclonic eddy in the oligotrophic North Pacific Ocean. *ISME J.* **2**, 663–676 (2008).
17. Liu, J. et al. Effect of mesoscale eddies on diazotroph community structure and nitrogen fixation rates in the South China Sea. *Regional Stud. Mar. Sci.* **35**, 101106 (2020).
18. Löscher, C. R. et al. N2 fixation in eddies of the eastern tropical South Pacific Ocean. *Biogeosciences* **13**, 2889–2899 (2016).
19. Wilson, S. T. et al. Coordinated regulation of growth, activity and transcription in natural populations of the unicellular nitrogen-fixing Cyanobacterium Crocosphaera. *Nat. Microbiol.* **2**, 17118 (2017).
20. Benavides, M. & Robidart, J. Bridging the spatiotemporal gap in diazotroph activity and diversity with high-resolution measurements. *Front. Marine Sci.* **7**, (2020). https://www.frontiersin.org/journals/marine-science/articles/10.3389/fmars.2022.877562/full.
21. Arístegui, J. et al. Island-induced eddies in the Canary Islands. *Deep Sea Res. Part I.* **41**, 1509–1525 (1994).
22. Piedeleu, M. et al. An observational study of oceanic eddy generation mechanisms by Tall Deep-Water Islands (gran canaria). *Geophys. Res. Lett.* **36**, 14 (2009).
23. Sangrà, P. et al. The canary eddy corridor: A major pathway for long-lived eddies in the subtropical North Atlantic. *Deep Sea Res. Part I.* **56**, 2100–2114 (2009).
24. Arístegui, J. et al. Sub-regional ecosystem variability in the Canary current upwelling. *Prog. Oceanogr.* **83**, 33–48 (2009).
25. Pelegrí, J. L. et al. Coupling between the open ocean and the coastal upwelling region off Northwest Africa: Water recirculation and offshore pumping of organic matter. *J. Mar. Syst.* **54**, 3–37 (2005).
26. Álvarez-Salgado, X. A. Contribution of upwelling filaments to offshore carbon export in the subtropical northeast Atlantic Ocean. *Limnol. Oceanogr.* **52**, 1287–1292 (2007).
27. Rahav, E., Giannetto, M. J. & Bar-Zeev, E. Contribution of mono and polysaccharides to heterotrophic N2 fixation at the eastern Mediterranean coastline. *Sci. Rep.* **6**, 27858 (2016).
28. Abraham, E. R. The generation of plankton patchiness by turbulent stirring. *Nature* **391**, 577–580 (1998).
29. Hörstmann, C. et al. Hydrographic fronts shape productivity, nitrogen fixation, and microbial community composition in the southern Indian Ocean and the Southern Ocean. *Biogeosciences* **18**, 3733–3749 (2021).
30. Hernández-Hernández, N. et al. Drivers of Plankton distribution across mesoscale eddies at Submesoscale Range. *Front. Marine Sci.* **7**, 667 (2020).
31. Cornejo-Castillo, F. M. et al. Metabolic trade-offs constrain the cell size ratio in a nitrogen-fixing symbiosis. *Cell*, **187**, 1762–1768.e9 (2024)
32. Coale, T. H. et al. Nitrogen-fixing organelle in a marine alga. *Science* **384**, 217–222 (2024).
33. Dugenne, M. et al. Nitrogen fixation in mesoscale eddies of the North Pacific Subtropical Gyre: Patterns and mechanisms. *Global Biogeochem. Cycles* **37**, e2022GB007386 (2023).
34. Robidart, J. C. et al. Ecogenomic sensor reveals controls on n2-fixing microorganisms in the North Pacific Ocean. *ISME J.* **8**, 1175–1185 (2014).
35. Agawin, N. S. et al. Dominance of unicellular cyanobacteria in the diazotrophic community in the Atlantic Ocean. *Limnol. Oceanogr.* **59**, 623–637 (2014).
36. Hallstrøm, S. et al. Pelagic n2 fixation dominated by sediment diazotrophic communities in a shallow temperate estuary. *Limnol. Oceanogr.* **67**, 364–378 (2021).
37. Breitbarth, E., Oschlies, A. & LaRoche, J. Physiological constraints on the global distribution of trichodesmium – effect of temperature on diazotrophy. *Biogeosciences* **4**, 53–61 (2007).
38. McGillicuddy, D. J. et al. Eddy/wind interactions stimulate extraordinary mid-ocean plankton blooms. *Science* **316**, 1021–1026 (2007).
39. Benavides, M. et al. Fine-scale sampling unveils diazotroph patchiness in the South Pacific Ocean. *ISME Commun.* **1**, 3 (2021).
40. Tyrrell, T. Large-scale latitudinal distribution of Trichodesmium spp. in the Atlantic Ocean. *J. Plankton Res.* **25**, 405–416 (2003).
41. Davis, C. S. & McGillicuddy, D. J. Transatlantic abundance of the N_2 fixing colonial cyanobacterium *Trichodesmium*. *Science* **312**, 1517–1520 (2006).
42. González Taboada, F., González Gil, R., Höfer, J., González, S. & Anadón, R. Trichodesmium spp. population structure in the eastern North Atlantic SubtropicalGyre. *Deep Sea Res. Part I.* **57**, 65–77 (2010).
43. Olson, E. M. et al. Mesoscale eddies and *trichodesmium* spp. distributions in the southwestern north atlantic. *J. Geophys. Res.Oceans* **120**, 4129–4150 (2015).
44. Palter, J. B. et al. High N2 fixation in and near the Gulf Stream consistent with a circulation control on diazotrophy. *Geophys. Res. Lett.* **47**, e2020GL089103 (2020).
45. Arístegui, J., Ramos, A. G. & Benavides, M. Informe sobre la presencia de *Trichodesmium* spp. en aguas de Canarias, en el verano de 2017. Technical Report, Gobierno de Canarias, Las Palmas de Gran Canaria, https://www3.gobiernodecanarias.org/sanidad/scs/content/cca93804-a35c-11e7-8b56-bf65dd086cd4/InformePresenciaTrichodesmiumspp.pdf (2017).
46. Benavides, M. et al. Sinking *trichodesmium* fixes nitrogen in the Dark Ocean. *ISME J.* **16**, 2398–2405 (2022).
47. Pabortsava, K. et al. Carbon sequestration in the Deep Atlantic enhanced by Saharan dust. *Nat. Geosci.* **10**, 189–194 (2017).
48. Villareal, T. A. & Carpenter, E. J. Buoyancy regulation and the potential for vertical migration in the Oceanic Cyanobacterium Trichodesmium. *Microb. Ecol.* **45**, 1–10 (2003).
49. Durkin, C. A., Van Mooy, B. A., Dyhrman, S. T. & Buesseler, K. O. Sinking phytoplankton associated with carbon flux in the Atlantic Ocean. *Limnol. Oceanogr.* **61**, 1172–1187 (2016).
50. Zhang, Y., Zhao, Z., Sun, J. & Jiao, N. Diversity and distribution of diazotrophic communities in the South China Sea deep basin with mesoscale cyclonic eddy perturbations. *FEMS Microbiol. Ecol.* **78**, 417–427 (2011).
51. Moisander, P. H. et al. Analogous nutrient limitations in unicellular diazotrophs and *Prochlorococcus* in the South Pacific Ocean. *ISME J.* **6**, 733–744 (2012).
52. Cerdán-García, E. et al. Transcriptional responses of *Trichodesmium* to natural inverse gradients of fe and P availability. *ISME J.* **16**, 1055–1064 (2022).
53. Oren, A. & Xu, X.-W. The family hyphomicrobiaceae. *Prokaryotes* 247–281. https://doi.org/10.1007/978-3-642-30197-1_257 (2014).
54. Yin, F. et al. Diversity of bacteria with quorum sensing and quenching activities from hydrothermal vents in the okinawa trough. *Microorganisms* **11**, 748 (2023).
55. Islam, T., Hernández, M., Gessesse, A., Murrell, J. C. & Øvreås, L. A novel moderately thermophilic facultative methylotroph within the class alphaproteobacteria. *Microorganisms* **9**, 477 (2021).
56. Avontuur, J. R. et al. Complex evolutionary history of photosynthesis in bradyrhizobium. *Microbial Genomics* **9**, https://doi.org/10.1099/mgen.0.001105 (2023).
57. Martínez-Pérez, C. et al. The small unicellular diazotrophic symbiont, UCYN-A, is a key player in the marine nitrogen cycle. *Nat. Microbiol.* **1**, 16163 (2016).

58. Waite, D. W. et al. Proposal to reclassify the proteobacterial classes Deltaproteobacteria and oligoflexia, and the phylum thermodesulfobacteria into four phyla reflecting major functional capabilities. *Int. J. Syst. Evolut. Microbiol.* **70**, 5972–6016 (2020).
59. Kapili, B. J., Barnett, S. E., Buckley, D. H. & Dekas, A. E. Evidence for phylogenetically and catabolically diverse active diazotrophs in deep-sea sediment. *ISME J.* **14**, 971–983 (2020).
60. Zehr, J. P. & Capone, D. G. Changing perspectives in marine nitrogen fixation. *Science* **368**, eaay9514 (2020).
61. Thompson, A. et al. Genetic diversity of the unicellular nitrogen-fixing cyanobacteria ucyn-a and its prymnesiophyte host. *Environ. Microbiol.* **16**, 3238–3249 (2014).
62. Cornejo-Castillo, F. M. & Zehr, J. P. Hopanoid lipids may facilitate aerobic nitrogen fixation in the Ocean. *Proc. Natl Acad. Sci.* **116**, 18269–18271 (2019).
63. Harding, K. J. et al. Cell-specific measurements show nitrogen fixation by particle-attached putative non-cyanobacterial diazotrophs in the North Pacific Subtropical Gyre. *Nat. Commun.* **13**, https://doi.org/10.1038/s41467-022-34585-y (2022).
64. Masuda, T. et al. Crocosphaeraas a major consumer of fixed nitrogen. *Microbiol. Spectrum* **10**, https://doi.org/10.1128/spectrum.02177-21 (2022).
65. Ratten, J.-M. et al. Sources of iron and phosphate affect the distribution of diazotrophs in the North Atlantic. *Deep Sea Res. Part II* **116**, 332–341 (2015).
66. Mark Moore, C. et al. Large-scale distribution of Atlantic nitrogen fixation controlled by Iron Availability. *Nat. Geosci.* **2**, 867–871 (2009).
67. Knapp, A. N. The sensitivity of Marine N2 fixation to dissolved inorganic nitrogen. *Front. Microbiol.* **3**, 374 (2012).
68. Inomura, K., Bragg, J., Riemann, L. & Follows, M. J. A quantitative model of nitrogen fixation in the presence of ammonium. *PLOS One* **13**, e0208282 (2018).
69. Moisander, P. H. et al. Chasing after non-cyanobacterial nitrogen fixation in marine pelagic environments. *Front. Microbiol.* **8**, 1736 (2017).
70. Mangolte, I., Lévy, M., Haëck, C. & Ohman, M. D. Sub-frontal niches of plankton communities driven by transport and trophic interactions at ocean fronts. *Biogeosciences* **20**, 3273–3299 (2023).
71. Mestre, M. et al. Sinking particles promote vertical connectivity in the ocean microbiome. *Proc. Natl Acad. Sci.*, **115**, E6799–E6807 (2018)
72. Wang, L., Gula, J., Collin, J. & Mémery, L. Effects of mesoscale dynamics on the path of fast-sinking particles to the Deep Ocean: A modeling study. *J. Geophys. Res.* **127**, e2022JC018799 (2022).
73. Lévy, M., Franks, P. J. & Smith, K. S. The role of submesoscale currents in Structuring Marine Ecosystems. *Nat. Commun.* **9**, 4758 (2018).
74. Della Penna, A. & Gaube, P. Mesoscale eddies structure mesopelagic communities. *Front. Marine Sci.* 7, https://doi.org/10.3389/fmars.2020.00454 (2020).
75. Le Moal, M., Collin, H. & Biegala, I. C. Intriguing diversity among diazotrophic picoplankton along a Mediterranean transect: A dominance of Rhizobia. *Biogeosciences* **8**, 827–840 (2011).
76. Álvarez–Salgado X. A. & Arístegui J. Organic matter dynamics in the Canary Current. In: *Oceanographic and Biological Features in the Canary Current Large Marine Ecosystem, Intergovernmental Oceanographic Commission Technical Series*, 115, chapter 3, pp. 151–159, http://hdl.handle.net/1834/9185 (2015).
77. Giering, S. L. et al. Sinking organic particles in the ocean—flux estimates from in situ optical devices. *Front. Marine Sci.* **6**, 834 (2020).
78. Ploug, H., Iversen, M. H., Koski, M. & Buitenhuis, E. T. Production, oxygen respiration rates, and sinking velocity of copepod fecal pellets: Direct measurements of ballasting by Opal and calcite. *Limnol. Oceanogr.* **53**, 469–476 (2008).
79. Ploug, H., Iversen, M. H. & Fischer, G. Ballast, sinking velocity, and apparent diffusivity within marine snow and zooplankton fecal pellets: Implications for substrate turnover by attached bacteria. *Limnol. Oceanogr.* **53**, 1878–1886 (2008).
80. Visser, A. & Jackson, G. Characteristics of the chemical plume behind a sinking particle in a turbulent water column. *Mar. Ecol. Prog. Ser.* **283**, 55–71 (2004).
81. Alonso-González, I. J. et al. Role of slowly settling particles in the ocean carbon cycle. *Geophys. Res. Lett.* **37**, 13 (2010).
82. Ababou, F. et al. Mechanistic understanding of diazotroph aggregation and sinking: "A rolling tank approach. *Limnol. Oceanogr.* **68**, 666–677 (2023).
83. Martínez-Moreno, J. et al. Global changes in oceanic mesoscale currents over the satellite altimetry record. *Nat. Clim. Change* **11**, 397–403 (2021).
84. Martínez-Marrero, A. et al. Near-inertial wave trapping near the base of an anticyclonic mesoscale eddy under normal atmospheric conditions. *J. Geophys. Res.* **124**, 8455–8467 (2019).
85. Fadeev, E. et al. Sea ice presence is linked to higher carbon export and vertical microbial connectivity in the Eurasian Arctic Ocean. *Commun. Biol.* **4**, 1255 (2021).
86. Valiente, S. et al. Dissolved and suspended organic matter dynamics in the Cape Verde Frontal Zone (NW Africa). *Prog. Oceanogr.* **201**, 102727 (2022).
87. Hansen, H. P. & Koroleff, F. Determination of nutrients. *Methods Seawater Anal.* 159–228, https://doi.org/10.1002/9783527613984.ch10 (1999).
88. Kérouel, R. & Aminot, A. Fluorometric determination of ammonia in sea and estuarine waters by direct segmented flow analysis. *Mar. Chem.* **57**, 265–275 (1997).
89. Zehr, J. P. & McReynolds, L. A. Use of degenerate oligonucleotides for amplification of the NIFH gene from the Marine Cyanobacterium Trichodesmium thiebautii. *Appl. Environ. Microbiol.* **55**, 2522–2526 (1989).
90. Callahan, B. J. et al. Dada2: High-resolution sample inference from Illumina Amplicon Data. *Nat. Methods* **13**, 581–583 (2016).
91. McMurdie, P. J. & Holmes, S. Phyloseq: An R package for reproducible interactive analysis and graphics of Microbiome Census Data. *PLoS One* **8**, e61217 (2013).
92. Oksanen, J. et al. vegan: Community Ecology Package. R package version 2.5-7, https://CRAN.R-project.org/package=vegan (2020).
93. Lahti L. & Shetty S. microbiome R package, https://doi.org/10.18129/B9.bioc.microbiome (2012–2019).
94. Kruskal, W. H. & Wallis, W. A. Use of ranks in one-Criterion Variance Analysis. *J. Am. Stat. Assoc.* **47**, 583–621 (1952).
95. Wilcoxon, F. Individual comparisons by ranking methods. *Biometrics Bull.* **1**, 80 (1945).
96. Love, M. I., Huber, W. & Anders, S. Moderated estimation of fold change and dispersion for RNA-seq data with deseq2, *Genome Biol.* 15, https://doi.org/10.1186/s13059-014-0550-8 (2014).

Acknowledgements

This research was funded by e-IMPACT project (PID2019-109084RB-C21 and -C22) from JA and XAAS supported by MCIN/AEI/10.13039/501100011033. X.A.A.S. and J.A. were also supported by project OceanICU (HORIZON-CL6-2022-CLIMATE-01-02; 101083922). Molecular work and sequencing were supported by the ANR-21-CE01-0032-01 project FIESTA from M.B. E.C.G. was financially supported by the French Ministry of Europe and Foreign Affairs within the MOPGA Campus France Fellowship Program (Fell. no. 126457X). The authors would like to thank the captain and crew of the B/O *Sarmiento de Gamboa*, as well as the Marine Technology Unit and scientific staff for their help during the cruise. We are particularly grateful to those who helped with the marine snow catcher deployment and processing and the members of the physics team Nadia Burgoa and Enedina. We also thank V. Vieitez for nutrient and M.J. Pazó for POM analyses.

Author contributions

E.C.G. and M.B. conceived and designed the study. E.C.G. and X.A.A.S. collected samples while at sea. E.C.G. processed the samples and analysed the sequence data. M.B. funded the analysis and molecular work. J.A. funded the cruise sampling. A.M.M. processed the physical analysis. X.A.A.S. processed the chemical analyses. E.C.G. wrote the manuscript, with significant contributions from M.B., X.A.A.S., A.M.M. and J.A. All authors contributed to data interpretation and editing of the paper.

Competing interests

The authors declare no competing interests.

Additional information

Supplementary information The online version contains supplementary material available at https://doi.org/10.1038/s42003-024-06576-w.

Correspondence and requests for materials should be addressed to E. Cerdán-García or M. Benavides.

Peer review information *Communications Biology* thanks François Delavat and the other, anonymous, reviewer(s) for their contribution to the peer review of this work. Primary Handling Editors: Linn Hoffmann and Tobias Goris. A peer review file is available.